

# The Static Baryon Potential

C. Alexandrou<sup>a\*</sup>, Ph. de Forcrand<sup>b</sup>, A. Tsapalis<sup>c†</sup>

<sup>a</sup>Department of Physics, University of Cyprus, CY-1678 Nicosia, Cyprus

<sup>b</sup>Institut für Theoretische Physik, ETH-Hönggerberg, CH-8093 Zürich, Switzerland and Theory Division, CERN, CH-1211 Geneva 23, Switzerland

<sup>c</sup>Department of Physics, University of Athens, Athens, Greece

Using state of the art lattice techniques we investigate the static baryon potential. We employ the multi-hit procedure for the time links and a variational approach to determine the ground state with sufficient accuracy that, for distances up to  $\sim 1.2$  fm, we can distinguish the  $Y$ - and  $\Delta$ - Ansätze for the baryonic Wilson area law. Our analysis shows that the  $\Delta$ -Ansatz is favoured. This result is also supported by the gauge-invariant nucleon wave function which we measure for the first time.

## 1. Introduction

Due to the important role which the  $q\bar{q}$  potential plays in our understanding of the structure of mesons, there exist numerous studies of this quantity on the lattice. For a review see ref. [1]. The three quark potential plays an equally important role in the understanding of baryon structure. Mass relations between baryons and mesons can be made more exact if the form of the baryonic potential is known [2]. However, very few lattice studies have been made of the baryonic potential. Moreover, two such recent studies [1,3] have reached different conclusions for the area law behaviour of the baryonic Wilson loop: they give support to two different Ansätze, called  $Y$ - and  $\Delta$ -law. Since the maximal difference between these is a mere 15% for  $SU(3)$ , a reliable extraction of the ground state as well as noise reduction techniques are essential in order to resolve the dominant area law behaviour [4].

In this work, employing state of the art lattice techniques, we are able to reach sufficient accuracy to distinguish between the two Ansätze up to distances of  $\sim 1.2$  fm. At the same time, we compare our lattice results directly to the sum of  $q\bar{q}$  potentials measured on the same lattices, thus avoiding any model assumptions. We also compare our procedure and results with those of

ref. [3] in order to understand the different conclusions reached.

The issue of the dominant area law behaviour arises for any gauge group  $SU(N)$ . Therefore it is also interesting to study  $SU(4)$  and test whether the  $SU(4)$  results corroborate the conclusions reached in  $SU(3)$ . As for  $SU(3)$ , we choose lattice geometries which maximize the difference between the two Ansätze which for  $SU(4)$  is at the 20% level.

As yet a further check, we evaluate the gauge-invariant nucleon wave function, using a density insertion for each quark line, and examine whether it is better described according to the  $Y$ - or  $\Delta$ - law [5].

## 2. Baryon Wilson loop

For the static  $q\bar{q}$  potential the appropriate operator is the standard Wilson loop. For the static baryon potential in  $SU(N)$ , the corresponding operator is constructed by creating a gauge invariant  $N$  quark state at time  $t = 0$  which is annihilated at a later time  $T$ . Explicitly for  $SU(3)$ , the baryon Wilson loop,  $W_{3q}$ , shown in Fig. 1, is given by

$$\frac{1}{3!} \epsilon^{abc} \epsilon^{a'b'c'} U(\mathbf{x}, \mathbf{y}, 1)^{aa'} U(\mathbf{x}, \mathbf{y}, 2)^{bb'} U(\mathbf{x}, \mathbf{y}, 3)^{cc'} \quad (1)$$

where

$$U(x, y, j) = P \exp \left[ ig \int_{\Gamma(j)} dx^\mu A_\mu(x) \right] \quad , \quad (2)$$

\*Talk presented by C. Alexandrou.

† Acknowledges funding from the University of Cyprus and the European network ESOP (HPRN-CT-2000-00130).

$P$  denotes path ordering and  $\Gamma(j)$  is the path from  $x$  to  $y$  for quark line  $j$ .

The  $N$ -quark potential is then extracted from the long time behaviour of the Wilson loop:

$$V_{Nq} = - \lim_{T \rightarrow \infty} \frac{1}{T} \ln \langle W_{Nq} \rangle \quad . \quad (3)$$

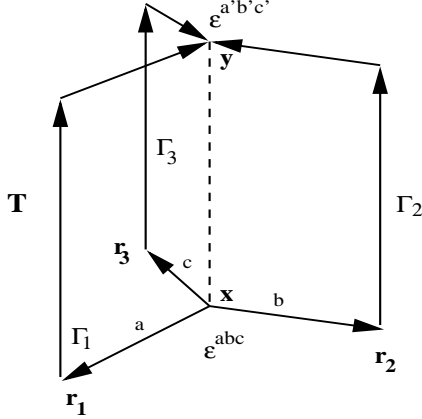


Figure 1. The baryonic Wilson loop in  $SU(3)$ . The quarks are located at positions  $\mathbf{r}_1, \mathbf{r}_2$  and  $\mathbf{r}_3$ .

### 3. Geometries in $SU(3)$ and $SU(4)$

Two Ansätze exist in the literature regarding the area law behaviour of the baryon Wilson loop:

- The  $Y$ -Ansatz:

In the strong coupling limit, minimization of the static energy amounts to giving the shortest length,  $L_Y$ , to the flux tubes joining the quarks. For  $SU(3)$ , this is realized in general if the three flux tubes meet at an interior point [6], known as the Steiner point, where their mutual angles are  $120^\circ$ . [If one of the angles of the triangle formed by the three quarks exceeds  $120^\circ$ , the flux tube coming from that summit has length zero, and the other two flux tubes meet there.] Time evolution of this state in the general case produces a three-bladed area similar to Fig.1, known as the  $Y$ - area law.

For  $SU(4)$  we have more possibilities. Minimization of the static energy leads to the two stationary solutions shown in Fig. 2, namely one configuration with a

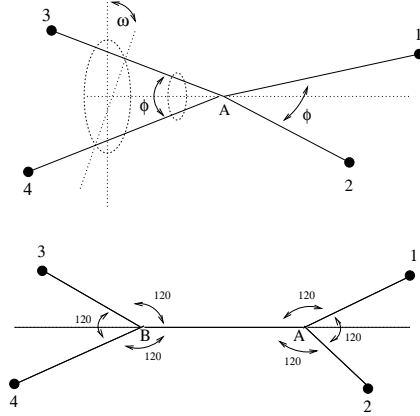


Figure 2. The flux tubes joining four quarks. The quarks are located at positions  $\mathbf{r}_1, \mathbf{r}_2, \mathbf{r}_3$  and  $\mathbf{r}_4$ . The upper graph shows the local minimum of the energy with one Steiner point A, and the lower is the minimum with two Steiner points A and B.

single Steiner point ( $X$ -Ansatz), and one with two Steiner points A and B ( $Y$ -Ansatz). The double string between the two Steiner points has tension 1.357(29) times greater[7] than the other four, single strings. If we neglect this difference for simplicity, then the  $Y$ -Ansatz always has lower energy than the  $X$ -Ansatz. Here, we make no attempt to distinguish between the  $Y$ - and  $X$ - Ansätze, and we assume that the double string has the same tension as the single strings. Since this assumption has the effect of reducing the potential of the  $Y$ -Ansatz, which is itself lower than in the  $X$ -Ansatz, it turns out to have no bearing on our conclusions. In contrast to  $SU(3)$  where for any given location of the three quarks, the Steiner point and therefore the  $Y$ -Ansatz energy can be computed analytically, in  $SU(4)$ , the two Steiner points in the  $Y$ -Ansatz are obtained by an iterative numerical procedure.

- The  $\Delta$ -Ansatz:

The second possibility for the relevant area dependence of the baryonic Wilson loop, proposed in ref. [8], is that it is given by the sum of the minimal areas  $A_{ij}$  spanning

quark lines  $i$  and  $j$ . Because of its shape in  $SU(3)$ , this Ansatz is known as the  $\Delta$ -area law. Therefore, we denote by  $L_\Delta$  the total length of all interquark distances.

For  $SU(3)$  the maximal difference of 15% between the two proposed area laws is obtained when the 3 quarks form an equilateral triangle.

For  $SU(4)$  it turns out that this relative difference is maximal also for the configuration of maximal symmetry among the four quarks. In this situation, where the quarks form a regular tetrahedron, it reaches 21.96 %. For programming convenience, we study instead the highly symmetric geometries shown in Fig. 3, which all give a relative difference of  $\sim 20\%$ .

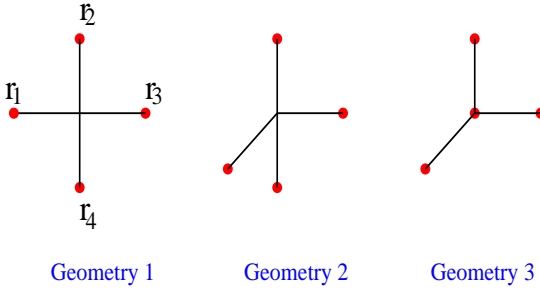


Figure 3. The geometries considered in  $SU(4)$ . For geometry 1 the quarks are placed on a plane at equal distances from the origin; for geometry 2 the positions of the four quarks are along the three axes at  $(1,0,0)$ ,  $(0,1,0)$ ,  $(0,0,1)$ ,  $(0,0,-1)$ ; and for geometry 3 at  $(0,0,0)$ ,  $(1,0,0)$ ,  $(0,1,0)$ ,  $(0,0,1)$ .

We compare our lattice results with the two expected forms of the baryonic potential which in  $SU(N)$  are

$$V_{Nq} = \frac{N}{2}V_0 - \frac{1}{N-1} \sum_{j < k} \frac{g^2 C_F}{4\pi r_{jk}} + \sigma \left\{ \frac{L_\Delta}{L_Y} \right\} \quad (4)$$

with  $C_F = (N^2 - 1)/2N$  and  $\sigma$  the string tension of the  $q\bar{q}$  potential. Note that in contrast to ref. [3] we do not allow  $\sigma$  to vary. The factor of  $1/(N-1)$  in the  $\Delta$ -Ansatz makes  $L_\Delta/(N-1) < L_Y$  always. In addition, we directly compare the three- or four-quark potential with the sum of two-body potentials measured on the same gauge configurations, with no adjustable parameters.

#### 4. Lattice techniques

**I. Multi-hit procedure:** We carried out a comparison between the multi-hit procedure and hypercubic-blocking, as proposed in ref. [9], for the time links. In brief, hypercubic blocking smears the link using staples which all belong to the  $2^4$  hypercube surrounding it. Compared with the multi-hit procedure, we find that hypercubic blocking tends to give larger errors, especially for the large Wilson loops. Since accuracy at large distances is our objective, we have adopted the multi-hit procedure. Moreover, for  $SU(3)$  the group integral needed to obtain the mean value of the link can be computed exactly [10]. We note that the reduction factor in the statistical error from applying the multi-hit procedure to Wilson loops of time extent  $t$  grows exponentially with  $t$ , and that the exponent is further multiplied by  $3/2$  in the case of baryonic loops.

**II. Smearing Correlation matrix:** We use a variational method to extract the groundstate potential. For each quark configuration, we consider  $M$  different levels of APE smearing, optimized as in ref. [11], and construct an  $M \times M$  correlation matrix  $C(t)$  of Wilson loops of time extent  $t$ . We then solve the generalized eigenvalue problem

$$C(t)v_k(t) = \lambda_k(t)C(t_0)v_k(t) \quad (5)$$

taking  $t_0/a = 1$ . We use two different methods to extract the groundstate energy:

1. In the first variant the potential is extracted via

$$aV_k = \lim_{t \rightarrow \infty} -\ln \left( \frac{\lambda_k(t+a)}{\lambda_k(t)} \right) \quad (6)$$

by fitting to the plateau. Note that with this method we also estimate the energy of the first excited state.

2. In the second variant we consider the projected Wilson loops

$$W_P(t) = v_0^T(t_0)C(t)v_0(t_0) \quad (7)$$

and fit to the plateau value of  $-\ln \left( W_P(t+1)/W_P(t) \right)$ . Both procedures gave consistent results. The energy of the first excited state was

used as a check in the extraction of the ground state, ensuring that the contamination is less than  $e^{-2}$  in the values considered for the plateau.

## 5. Results

For the baryonic loop in  $SU(3)$  we used 220 configurations at  $\beta = 5.8$  and 200 at  $\beta = 6.0$  for a lattice of size  $16^3 \times 32$  from the NERSC archive. For  $SU(4)$  we generated 100 configurations at  $\beta = 10.9$  which gives a similar string tension  $\sigma a^2$  as for  $SU(3)$  at  $\beta = 6.0$ .

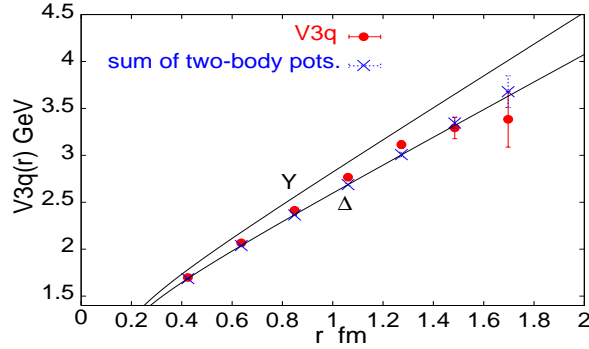


Figure 4. The static  $SU(3)$  baryonic potential at  $\beta = 5.8$  (filled circles). The crosses show the sum of the static  $q\bar{q}$  potentials. The curves for the  $\Delta$  and  $Y$  Ansätze are also displayed. The quarks are located at  $(l, 0, 0)$ ,  $(0, l, 0)$ ,  $(0, 0, l)$  and  $r = r_{12} = r_{13} = r_{23} = l\sqrt{2}$ .

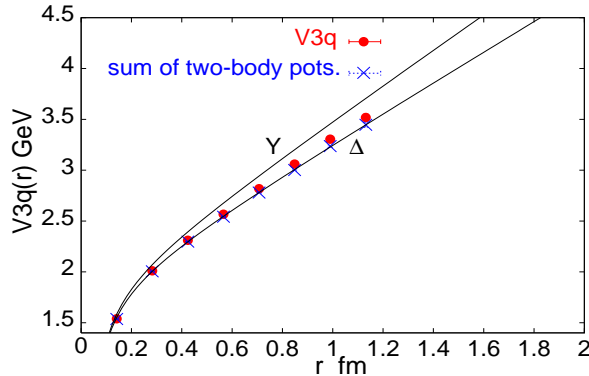


Figure 5. As Figure 4 but for  $\beta = 6.0$ .

The results at  $\beta = 5.8$  and  $6.0$  show reasonable scaling and are completely consistent with

the sum of  $q\bar{q}$  potentials extracted from measurements on the same lattices, i.e. we find  $V_{3q} \approx 3/2 V_{q\bar{q}}$ , in agreement with ref. [1].

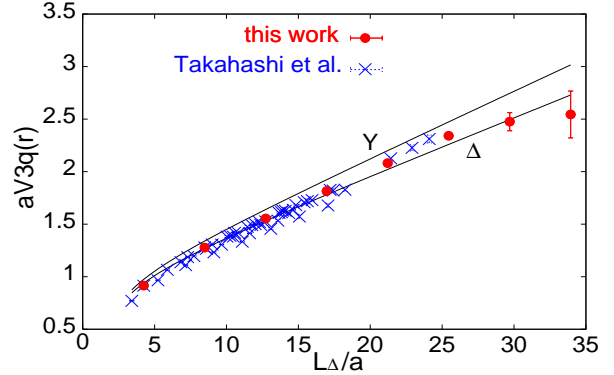


Figure 6. The static  $SU(3)$  baryonic potential at  $\beta = 5.8$  for this work (filled circles) and for ref. [12] (crosses) versus the perimeter  $L_\Delta$  of the triangle formed by the quarks.

In Fig. 6 we compare our results with those obtained in ref. [12]. As it can be seen the two sets of data are in agreement for small loops which correspond to the bulk of the data of ref. [12]. For larger loops, the few results of ref. [12] tend to lie above ours. The statistical errors on these data are not quoted but we expect them to be larger than ours, especially since the multi-hit procedure was not used. The analysis of ref. [12] differs from ours in that we do not allow the string tension to vary but take it from the fit to the  $q\bar{q}$  potential. So in our approach having fixed the  $q\bar{q}$  potential there are no adjustable parameters that enter in the two Ansätze.

Additional support for the  $\Delta$ -Ansatz is provided by preliminary results on the gauge-invariant nucleon wave function, obtained by inserting three density operators at an intermediate time  $t$  along the three quark lines of a baryon propagator. In Fig. 7 we plot the wave function versus  $L_Y$  and  $L_\Delta/2$ . We observe a larger scatter when  $L_Y$  is used as compared to  $L_\Delta$ . The nucleon wave function plotted versus  $L_\Delta$  is displayed together with a fit to the form  $\exp(-cL_\Delta^{3/2})$ , expected if the underlying potential is  $\propto L_\Delta$ . As

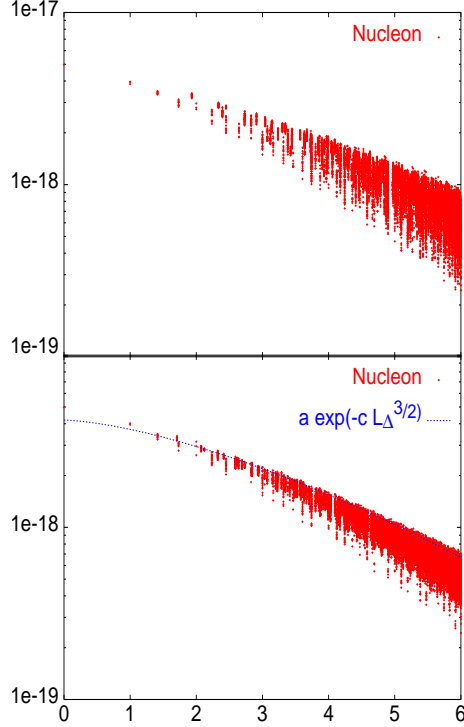


Figure 7. Upper graph: The nucleon wave function versus  $L_Y$ . Lower graph: The nucleon wave function versus  $L_\Delta/2$ , fitted by a linear potential ansatz. All quantities are in lattice units.

can be seen, this simple asymptotic form provides a remarkably good description of the nucleon wave function.

Finally we display the results obtained in  $SU(4)$  for geometry 3. They give yet more support to the  $\Delta$ -area law for the baryon Wilson loop. The other two geometries show the same behaviour.

## 6. Conclusions

Our results for the static three- and four-quark potential in  $SU(3)$  and  $SU(4)$  are consistent with the sum of two-body potentials and inconsistent with the  $Y$ -Ansatz up to an interquark distance of about 0.8 fm. For larger distances, where our statistical and systematic errors both become appreciable, there appears to be a small enhancement which could be assigned to the admixture

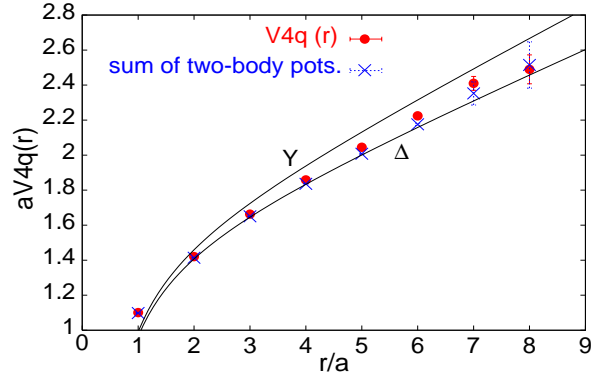


Figure 8. The static  $SU(4)$  baryonic potential in lattice units for geometry 3.

of a many-body component. Nevertheless, for the distances up to 1.2 fm that we were able to probe in this work, the  $\Delta$ -area law gives the closest description of our data. More refined noise-reduction techniques for the large loops will be needed in order to clarify or rule out a many-body component at larger distances. Preliminary results on the nucleon wavefunction also support a potential in accord with the  $\Delta$ -Ansatz.

## REFERENCES

1. G. S. Bali, Phys. Rept. **343** (2001) 1.
2. S. Nussinov, Phys. Rev. Lett. **51** (1983) 2081; T. D. Imbo, Phys. Lett. B **398** (1997) 374.
3. T. T. Takahashi *et al.*, Phys. Rev. Lett. **86** (2001) 18.
4. C. Alexandrou, Ph. de Forcrand and A. Tsapalis, hep-lat/0107006.
5. C. Alexandrou, Ph. de Forcrand and A. Tsapalis, in preparation.
6. J. Carlson, J. Kogut and V. R. Pandharipande, Phys. Rev. D **27** (1983) 233.
7. B. Lucini and M. Teper, hep-lat/0107007.
8. J. M. Cornwall, Phys. Rev. D **54** (1996) 6527.
9. A. Hasenfratz and F. Knechtli, hep-lat/0103029.
10. Ph. de Forcrand and C. Roiesnel, Phys. Lett. B **151** (1985) 77.
11. M. Guagnelli, R. Sommer and H. Wittig, Nucl. Phys. B **535** (1998) 389.
12. T. T. Takahashi *et al.*, hep-lat/0107008.